ASM Sc. J., 19, 2024

https://doi.org/10.32802/asmscj.2023.1518

Spectral Variation of Normalised Laplacian for Various Network Models

Y.S.J. Liang[1], K.T. Chan[1,2*] and N.M. Shah[1,2]

[1]*Laboratory of Computational Sciences and Mathematical Physics, Institute for Mathematical Research (INSPEM), 43400 UPM Serdang, Selangor, Malaysia*

[2]*Department of Physics, Faculty of Science, Universiti Putra Malaysia, 43400 UPM Serdang, Selangor, Malaysia*

Many network models have been proposed to mimic real-world systems when they become too large and complex to be described explicitly. Since the models inherit similar structural properties to the real-world network, by studying their nodes and links, many network properties can be identified. While most of the tools used to study their structural properties are coming from graph theory, spectral analysis is another method that can be used to reveal the structural inheritance properties of a network. In this work, we performed spectral analysis on network models, namely Erdo-Renyi (ER), Watts-Strogatz (WS), Barabasi Albert (BA), grids and growing geometrical network (GGN) with the undirected and directed connection. The eigenvalue spectrum of the normalised Laplacian was computed for each model and used in spectral plots, Cheeger constant and energy measurement. Results from the spectral measures have revealed specific characteristics for different models, which in turn make them easier to be recognised.

Keywords: Normalised Laplacian; Spectral analysis; Complex network

I. INTRODUCTION

A network is a simplified representation of a complex system where the entities of the system are represented by the nodes and their relationships are represented by the edges that connect them. In recent years, the study of complex networks has been on the rise as more and more complex systems ranging from technical to biological have been successfully constructed, modelled, and analysed. Some of the well-known examples are the World Wide Web (Liang *et al.*,2019), the Internet (Pantazopoulos, 2015), protein-protein interaction (Andreopoulos *et al.*, 2003), the online social network (Mislove, 2009) and the network of medicine by Barabasi (Barabasi & Albert, 1999).

Network theory which is a part of graph theory played a vital role in developing measurement (i.e. parameter) to analyse the inheritance structural properties of the network such as degree distribution (Newman, 2010), average path length (Pattanayak *et al.*, 2020), diameter, centrality analysis and clustering coefficient (Li *et al.*, 2017). Research in network science which focused on understanding the topological structure of the underlying networks (Ernesto *et al.*, 2009) has led to the basic understanding of emergent phenomena in various complex systems and processes such as disease spreading, scientific collaboration, communities detection and cellular signalling (Sarkar & Jalan, 2018). Since complex networks usually involve thousands of nodes, many network models have been proposed and constructed to mimic the underlying features of complex networks for instance Erdo-Renyi (ER) (Erdos & Renyi, 1959), Watts-Strogatz (WS) (Watts & Strogatz, 1998), Barabasi Albert (BA) (Barabasi & Albert, 1999) and growing geometrical network (GGN) model (Taha *et al.*, 2016).

In recent years, researchers have started to analyse the inheritance properties using spectral graph theory or just spectral studies (Polya & Szego, 1951.) This method has been used as a tool to establish the relationship between various properties of a graph and the characteristic polynomial, eigenvalues, and eigenvectors of connectivity matrices

*Corresponding author's e-mail: chankt@upm.edu.my

associated with the graph (Li & Zhang, 2015). The spectrum of the associated eigenvalues of the networks contains valuable information about the structural characteristics of underlying networks and also provides insight into the dynamical behaviour and stability of corresponding complex systems (Chung, 1997). Since different networks will have different sets of spectra, this convenience can be utilised as a practical tool for classifying and understanding different real-world systems represented as networks (Sarkar & Jalan, 2018).

Traditionally, the study of networks focused on regular graphs. As systems now have become more complex or involve thousands to millions of nodes as in most of real-world networks, many models have been proposed by researchers to mimic them. One of the earliest network models was the random network model introduced by the Erdos-Renyi in 1959. This network model generates a network with a certain probability (Erdos & Renyi, 1959). This model has been the cornerstone for many scientific discoveries and notable results (Castro & Grossman, 1999). The next BA scale-free network has growth preference attachment and the BA network model is invented by Albert-Laszlo Barabasi and Reka Albert in 1999 (Barabasi & Albert, 1999). WS small work network has a low average path length and high clustering coefficient (Watts & Strogatz, 1998). Then the grid network models, i.e. square grid and triangular grid were introduced by Eric Weisstein (2001). Square grid is a two-dimensional grid graph whereas triangular grid is defined as an induced subgraph of a tiling plane with equilateral triangles. Lastly, the growing geometrical network model is the study of the evolving network. GGN network is built with a certain shape; when the number of the iteration increases, the number of nodes increases based on the repeating structure and shape (Wu *et al*., 2014).

In this paper, we investigate the spectrum of normalised Laplacian for the network with undirected or directed connections for six different models namely, ER random network, BA scale-free, WS small world, square regular (S_{grid}) network, triangular grid lattice (T_{grid}) network and GGN models. This work aims to analyse and compare the spectral properties of the network models computed from spectral plots, Cheeger constant and energy measurement to reveal their specific characteristics which in turn make them easier to be recognised. All the computation and network model construction are performed using Mathematica software. It is important to differentiate the models and their characteristics in real applications because real-world networks are too large to describe explicitly and direct visualisation is only applicable when the network is sparse or only involves a small number of nodes. It will be too complicated for the eye to comprehend if the network goes up to a few thousand nodes.

These models will attempt to mimic the real-world network construction processes to reproduce similar inheritance structural properties. Various parameters, such as degree distribution, average path length, diameter, betweenness centrality, transitivity or clustering coefficient (Newman, 2004), are measured from the networks to perform further studies. In addition, Banerjee (2008) has constructed many networks to analyse the structural inheritance properties of a network. Via these kinds of characterisation, it is found that networks that share common properties are usually similar in their topological structure.

II. FUNDAMENTAL AND METHODOLOGY

B. Connectivity Matrices

A connectivity matrix (or adjacency matrix ($A(G)$)) is a matrix that shows how the nodes in a network are connected. The two commonly used connectivity matrices associated with the network are the Laplacian matrix ($L(G)$) and the normalised Laplacian matrix ($NL(G)$).

The equation for the $A(G)$ is given as:

$$A_{ij} = \begin{cases} 1 & if\ there\ is\ an\ edge\ between\ node\ i\ and\ j, \\ 0 & otherwise. \end{cases} \quad (1)$$

As for the $L(G)$, the equation is given as

$$L_{ij} = \begin{cases} d(i) & if\ i = j, \\ -1 & if\ i \neq j\ and\ there\ is\ an\ edge\ between\ i\ and\ j, \\ 0 & otherwise. \end{cases} \quad (2)$$

where $d(i)$ is the degree of node i.

The equation for the *NL(G)* (Butler, 2016) is

$$NL_{ij} \tag{3}$$

$$= \begin{cases} -\frac{1}{\sqrt{d(i)d(j)}} & if\ i \neq j\ and\ i \sim j, \\ \frac{d(i)-1}{d(i)} & if\ i = j\ and\ d(i) \neq 0, \\ 0 & otherwise. \end{cases} \tag{4}$$

where *d(j)* is the degree of the node j.

The *L(G)* and *NL(G)* are related to the *A(G)* via Equations 4 and 5 respectively:

$$L = D - A, \tag{4}$$

$$NL = I - D^{-1/2}AD^{-1/2} \tag{5}$$

where D is the diagonal matrix, I is the identity matrix and A is the adjacency matrix.

B. Normalised Laplacian Spectral Density Plot (NLSDP)

In order to study the properties of the network models, the normalised Laplacian spectrum is utilised to plot the spectral density plot. The spectral density of a network is the density of the eigenvalues of $NL(G)$. For a finite system, this can be written as the sum of delta function given as (Chung, 1997)

$$p(\lambda) \equiv \frac{1}{n}\sum_{j=1}^{n} \delta(\lambda - \lambda_j), \tag{6}$$

where n is the number of nodes, $\delta(\lambda - \lambda_j)$ is the Kroneker delta function for the spectrum of the network model.

C. Cheeger Constant

Cheeger constant (h_G) of a graph is a numerical measure of whether or not a graph has a bottleneck (a point where the system is limited by connection). h_G is measured to identify the bottleneck of the network. Cheeger constant of a subset S is defined as

$$h_G(S) = \frac{\left|E(S,\overline{S})\right|}{\min(volS, vol\overline{S})} \tag{7}$$

where $\left|E(S,\overline{S})\right|$ denotes the set of edges linking to subset S and $\overline{S}$.

h_G of a graph, G is defined as

$$h_G = \min_G(h_G(S)) \tag{8}$$

which means we need to choose the smallest possible h_G value. h_G also satisfied the Cheeger inequality, which is the relationship between the h_G and the second smallest eigenvalue (λ_2), which Cheeger inequality is given as

$$\frac{1}{2}h_G^2 \leq \lambda_2 \leq 2h_G \tag{9}$$

D. Energy

Energy is the sum of the absolute eigenvalues of a network. The adjacency energy ($E_A(G)$) is defined as

$$E_A(G) = \sum_{i=1}^{n} |\lambda_i(A)| \tag{10}$$

where n represents the order of the network and $\lambda_i(A)$ is the eigenvalues for $A(G)$.

As for the energy of the directed network (or digraph, $\bar{G}$), $\lambda_i(A)$ is replaced with $\mathrm{Re}\,\lambda_i$ which is the real part of eigenvalues λ_i (Rada, 2009). When we considered $NL(G)$, the normalised Laplacian energy ($E_{NL}(G)$) is given as,

$$E_{NL}(G) = \sum_{i=1}^{n} |\lambda_i(NL) - 1| \tag{11}$$

where $\lambda_i(NL)$ is the eigenvalues for $NL(G)$.

For an N-nodes complete network, if we are using *A(G)* the analytical energy is given by $E(K_n) = 2(n-1)$ (Balakrishnan, 2004) where K_n refer to the complete network while if we are using *NL(G)*, the energy is two (Cavers et al., 2010). The ratio R_{AM}, between the $E_A(G)$ of the network model and the complete network is then computed to describe the network's structure. If the ratio is one, this means that the network model is a complete network. If the value is small, it means that nodes are sparsely connected.

For $E_{NL}(G)$, we take the ratio R_{NL} between the energy of the network model with the upper bound of the energy spectrum (Cavers et al., 2010) which is defined as

$$2 \leq E_{NL}(G) \leq 2\left\lfloor\frac{n}{2}\right\rfloor \tag{12}$$

$$1 \leq E_{NL}(\bar{G}) \leq \left\lfloor\frac{n}{2}\right\rfloor \tag{13}$$

where $\left\lfloor\frac{n}{2}\right\rfloor$ is the floor function that rounds down and returns the largest integer less than or equal to a given number.

E. Construction of Network Based on Different Network Models

In network study, network models are developed to mimic real-world systems. They are important because the pattern and properties determined from them using spectral analysis

can be used to characterise complex real-world networks. Different network models are generated using different algorithms. In this section, we explain how all the network models are generated using Mathematica software.

ER random graph model is represented as $G(n,p)$ (Erdos & Renyi, 1959) where n is the number of nodes and p is the probability. According to Erdos and Renyi (1959), the algorithm for constructing this network model is as follows:

i. First, input n and p for the network. Based on these values, the number of edges $m = p\frac{n(n-1)}{2}$ is computed.

ii. A pair of randomly selected nodes is chosen and an edge is added with probability p.

iii. Step ii. is repeated until it reached the number of edges determined in step i.

A minor modification is applied when generated in Mathematica where p is replaced with m such that the random graph is $G(n,m)$. For directed network, an additional command as shown in Figure 1 is used.

```
Print["Number of Nodes,n = ", n = 500]
Print["Probability,p = ", p = 0.2]
m = IntegerPart[p (n (n - 1) / 2)];

REgraph = RandomGraph[{n, m}, VertexStyle → Green,
   VertexLabels → {"Name"}]
Print["Number of Edges,m = ", EdgeCount[REgraph]]

dREgraph = DirectedGraph[REgraph, "Random"]
Print["Number of Edges,m = ", EdgeCount[dREgraph]]
Number of Nodes,n = 500
Probability,p = 0.2
```

Figure 1. Command used to construct undirected and directed ER models

WS small-world graph model is represented as $G(n,p,k)$ (Watts & Strogatz, 1998). According to Watts and Strogatz, (1998), the algorithm for constructing this network model is as follows:

i. Input the number of n, p and the number of ranges connecting to the nearest neighbour, k.

ii. A network with n is generated and each node is connected.

iii. A nearest clockwise neighbour node is chosen to form an edge.

iv. The edge followed the p for rewiring and reconnected to a chosen node randomly, or else, the edge is not connected to any node.

v. Steps iii. to iv. are repeated around a circle till one lap is completed.

vi. Then next lap is repeated untill k number of laps.

For the directed graph, it is built by directing the undirected edges randomly. The algorithm is shown in Figure 2.

```
Print["Number of Nodes,n = ", n = 100]
Print["Rewiring Probability,p = ", p = 0.2]
Print["Range,k = ", k = 2]
WSgraph =
 RandomGraph[WattsStrogatzGraphDistribution[n, p, k],
  VertexStyle → Green, VertexLabels → {"Name"}]
Print["Number of Edges,m = ", EdgeCount[WSgraph]]

dWSgraph = DirectedGraph[WSgraph, "Random"]
Print["Number of Edges,m = ", EdgeCount[dWSgraph]]
Number of Nodes,n = 100
Rewiring Probability,p = 0.2
Range,k = 2
```

Figure 2. Command used to construct undirected and directed WS network models

The BA network model is represented as $G(n,l)$ where n is the number of nodes and l is the number of new edges connected per added node (Barabasi & Albert, 1999). The algorithm for constructing this network model is shown below:

i. Input number of n and l.

ii. Initially, a two nodes graph with an edge is formed.

iii. When a new node is added, l edges are added to the selected nodes based on preferential attachment. The algorithm is shown in Figure 3.

```
Print["Number of Nodes,n = ", n = 500]
Print["Number of new edges connected per added node,l = ",
 l = 2]
BAgraph = RandomGraph[BarabasiAlbertGraphDistribution[n, l],
   VertexStyle → Green, VertexLabels → {"Name"}]
Print["Number of Edges,m = ", EdgeCount[BAgraph]]

dBAgraph = DirectedGraph[BAgraph, "Random"]
Print["Number of Edges,m = ", EdgeCount[dBAgraph]]
Number of Nodes,n = 500
Number of new edges connected per added node,l = 2
```

Figure 3. Command used to construct undirected and directed BA network models

The S_{grid} network model can be constructed in Mathematica by using function $GridGraph(h,w)$ where h represented the height and w represented the width. To implement the direction in this model, we use *'DirectedGraph'* command and the code for this model is shown in Figure 4.

```
g = GridGraph[{10, 50}, VertexLabels → {"Name"}]

g2 = DirectedGraph[g, "Random"]
```

Figure 4. Command used to construct undirected and directed S_{grid} network model

The T_{grid} network model is represented as $TriangularGridGraph(n_i)$ where n_i represented the number of iterations for generating the triangular grid graph's nodes. $TriangularGridGraph(n_i)$ is a module available in Mathematica as shown in Figure 5.

```
TriangularGridGraph[n0_] := Module[{i, j, v, e, tab, n = n0 + 1},
  v = Table[{i - j / 2, -j Sqrt[3] / 2}, {j, n}, {i, j}];
  tab = Table[Range[i (i - 1) / 2 + 1, i (i + 1) / 2], {i, n}];
  e =
   Union[
    Flatten[
     {Transpose[{#[[1]], Most[#[[2]]]}],
        Transpose[{#[[1]], Rest[#[[2]]]}]} & /@
      Partition[tab, 2, 1], 2],
    Flatten[Partition[#, 2, 1] & /@ tab, 1]];
  System`Graph[Range[Binomial[n, 2]], UndirectedEdge @@@ e,
   VertexCoordinates -> Flatten[v, 1],
   VertexLabels → {"Name"}]]

tgg = TriangularGridGraph[44]
VertexCount[tgg]
DirectedGraph[tgg, "Random"]
```

Figure 5. Command used to construct undirected and directed T_{grid} network model

The growing geometrical network model is constructed based on the tessellation of hyperbolic triangle as shown in Figure 6 (Taha *et al.*, 2016) on a hyperbolic plane. This kind of tringle are generated by two orientation preserving generators and the sum of its angle is less than 180°. For this work, hyperbolic triangle $T(2,6,4)$ is used. The GGN network model is grown by iterating the given tessellation. Part of the command is shown in Figure 7.

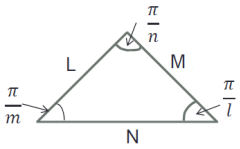

Figure 6. Hyperbolic Triangle, *T(n,m,l)* where L, M and N are the edges of the triangle

```
Unprotect[NonCommutativeMultiply];
s ** s = t ** t ** t ** t ** t =
   s ** t ** s ** t ** s ** t ** s ** t = e;
e ** w_ = w_ ** e = w;
Format[NonCommutativeMultiply[s___]] := SequenceForm[s]
SetAttributes[NonCommutativeMultiply,
 {Protected, Listable}]

s ** t ** s ** t ** s ** t ** s ** t; s ** t ** s;
s ** t ** s ** t ** s ** t ** s ** t;

α = π/6; β = π/4; p = ((Cos[β])^2 - (Sin[α])^2)^0.5;

xq = (Cos[β] - Sin[α])/p; xp = (Cos[α] * Cos[α + β])/p;
yp = (Sin[α] * Cos[α + β])/p;

Attributes[groupExtend] = Listable;
groupExtend[(x___ : e) ** s] := x ** s ** t;
groupExtend[(x___ : e) ** t] := x ** t ** {s, t};
groupExtend[(x___) ** t ** t ** t ** t ** t] :=
  x ** t ** t ** t ** t ** s;
groupExtend[(x___) ** s ** t ** s ** t ** s ** t ** s] :=
 x ** s ** t ** s ** t ** s ** t ** s ** t ** {s, t}
groupExtend[e] = {s, t};

Trace[NestList[groupExtend, e, 2]];

G = Union[Flatten[NestList[groupExtend, e, 7]]]
```

Figure 7. Command used to construct undirected and directed GGN network model

III. RESULT AND DISCUSSION

A. Visualisation of the Constructed Network Models

Visualisation of undirected and directed network models with n =100 generated using Mathematica are shown in Figure 8. As for T_{grid} and GGN networks, 105 and 116 nodes are used for the visualisation because their construction depends on the different number of tessellation where each tesselation are related to the number of iterations. From the figure, different models display very different topological structures. The structure will become more complex and challenging to identify as the number of nodes increases.

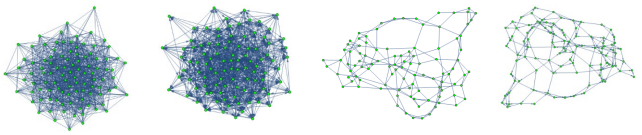

(a) 100 nodes ER (b) 100 nodes WS

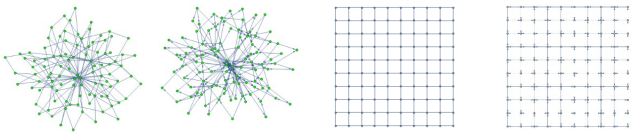

(c) 100 nodes BA (d) 100 nodes S_{grid}

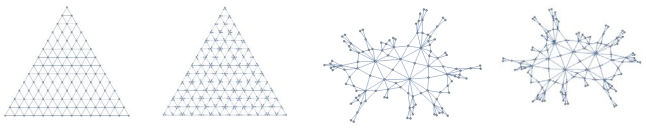

e) 105 nodes T_{grid} f) 116 nodes GGN

Figure 8. The Topological Structure of Undirected (left) and Directed (right) Network Models

B. Basic Measures

As complexity increases, it will be difficult to identify some basic properties of the network such as the number of nodes, the number of degrees and the number of edges. Performing some basic measures on this network can provide some crucial information for the networks. The results of the basic measures of the undirected and directed network models are shown in Table 1 and Table 2 respectively.

Generally, as the number of nodes increases, the mean degree and average path length for most of the models' increases while their density decreases. However, there are few exceptions. It is found that the density of the undirected and directed ER network models remained constant. This is because the computed density is similar to the probability set in the algorithm for ER model. The mean degree for WS model in both connections is also constant. This is again due to the algorithm for generating the WS network where we have set the node to be connected to two nearest neighbours.

For the average clustering coefficient, one important piece of information we get is that S_{grid} recorded zero value for both network connections. This is because S_{grid} models do not form cliques (triplets of nodes) with their neighbours as required in clustering coefficient measurement.

C. Normalised Laplacian Spectral Density Plot (NLSDP)

The spectrum properties vary among network models of different sizes and become an important factor for network characterisation. NLSDP has a certain advantage compared to plots from *A(G)* and *L(G)* because the spectrum is bounded within eigenvalues [0, 2] hence making it easy for comparison. Besides, the spectrum of the *NL(G)* also reflects the global properties of the network (Banerjee, 2008). Results from the NLSDP for the six undirected and directed network models are shown in Figure 10.

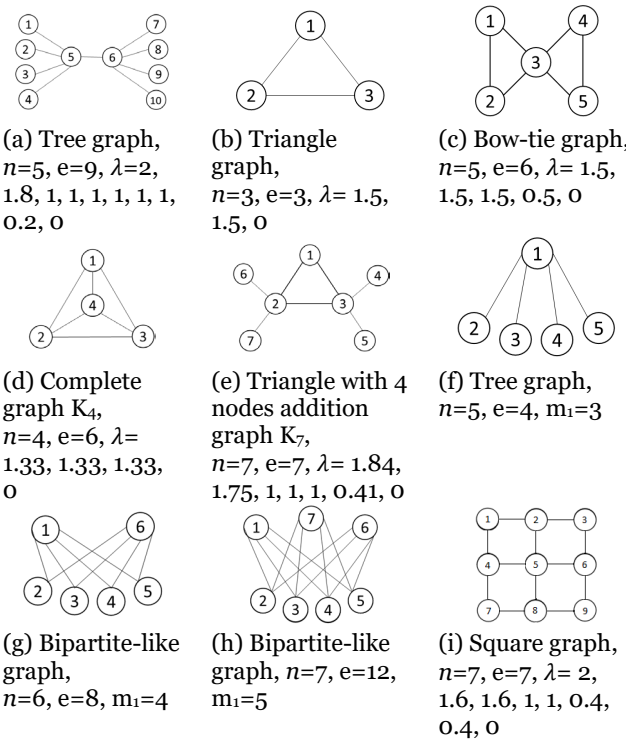

(a) Tree graph, n=5, e=9, λ=2, 1.8, 1, 1, 1, 1, 1, 0.2, 0

(b) Triangle graph, n=3, e=3, λ= 1.5, 1.5, 0

(c) Bow-tie graph, n=5, e=6, λ= 1.5, 1.5, 1.5, 0.5, 0

(d) Complete graph K_4, n=4, e=6, λ= 1.33, 1.33, 1.33, 0

(e) Triangle with 4 nodes addition graph K_7, n=7, e=7, λ= 1.84, 1.75, 1, 1, 1, 0.41, 0

(f) Tree graph, n=5, e=4, m_1=3

(g) Bipartite-like graph, n=6, e=8, m_1=4

(h) Bipartite-like graph, n=7, e=12, m_1=5

(i) Square graph, n=7, e=7, λ= 2, 1.6, 1.6, 1, 1, 0.4, 0.4, 0

Figure 9. Motifs for undirected networks (n=number of nodes, e=number of edges, λ=eigenvalues and m_1=multiplicity of eigenvalue 1)

Table 1. Basic measures for directed network models

Network Models	Number of Vertex	Number of Edges	Density	Total number of Degree	Mean Degree	Total number of In-Degree	Mean In-Degree	Total number of Out-Degree	Mean Out-Degree	Mean Deviation	Average Path Length	Average Clustering Coefficient
ER	100	990	0.10	1980	19.80	990	9.90	990	9.90	2.91	2.25	0.10
	300	8970	0.10	17940	59.80	8970	29.90	8975	29.90	5.49	1.94	0.10
	500	24950	0.10	49900	99.80	24950	49.90	24950	49.90	7.03	1.91	0.10
	1000	99900	0.10	199800	199.80	99900	99.90	99900	99.90	9.80	1.90	0.10
WS	100	200	0.02	400	4.00	200	2.00	200	2.00	0.66	7.50	0.06
	300	600	0.01	1200	4.00	600	2.00	600	2.00	0.61	11.25	0.09
	500	1000	0.00401	2000	4.00	1000	2.00	1000	2.00	0.58	14.95	0.11
	1000	2000	0.00200	4000	4.00	2000	2.00	2000	2.00	0.49	15.67	0.11
BA	100	197	0.02	394	3.94	197	1.97	197	1.97	2.18	4.44	0.10
	300	597	0.01	1194	3.98	597	1.99	597	1.99	2.37	5.39	0.03

	500	997	0.00400	1994	3.99	997	1.99	997	1.99	2.40	5.44	0.02
	1000	1997	0.00200	3994	3.99	1997	2.00	1997	2.00	2.34	6.30	0.00
S_{grid}	100	180	0.02	360	3.60	180	1.80	180	1.80	0.51	8.71	0.00
	300	560	0.01	1120	3.73	560	1.87	560	1.87	0.40	13.63	0.00
	500	940	0.00377	1880	3.76	940	1.88	940	1.88	0.37	13.06	0.00
	1000	1890	0.00189	3780	3.78	1890	1.89	1890	1.89	0.35	17.22	0.00
T_{grid}	105	273	0.03	546	5.20	273	2.60	273	2.60	1.01	3.00	0.22
	210	570	0.01	1140	5.43	570	2.71	570	2.71	0.83	3.38	0.17
	528	1488	0.01	2976	5.64	1488	2.82	1488	2.82	0.60	3.91	0.19
	1035	2970	0.00278	5940	5.74	2970	2.87	2970	2.87	0.46	4.30	0.19
GGN	116	228	0.02	456	3.93	228	1.97	228	1.97	1.50	3.52	0.20
	373	762	0.01	1524	4.09	726	2.04	726	2.04	0.00	4.24	0.20
	545	1116	0.00376	2232	4.10	1116	2.05	1116	2.05	1.63	4.50	0.22
	1150	2376	0.00180	4752	4.13	2376	2.07	2376	2.07	1.66	4.97	0.22

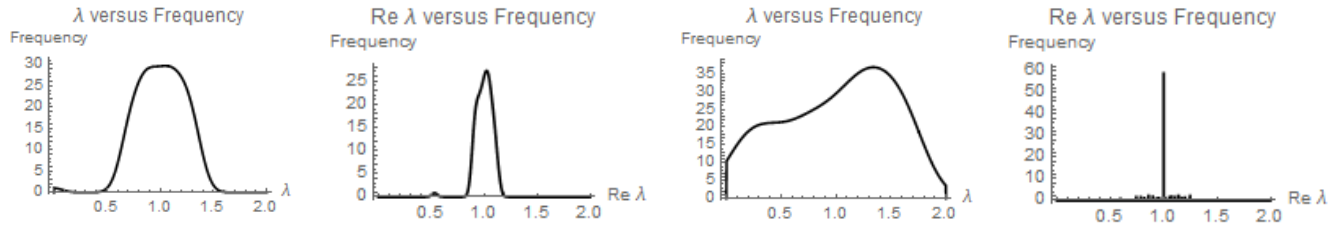

(a) 100 nodes ER

(b) 100 nodes WS

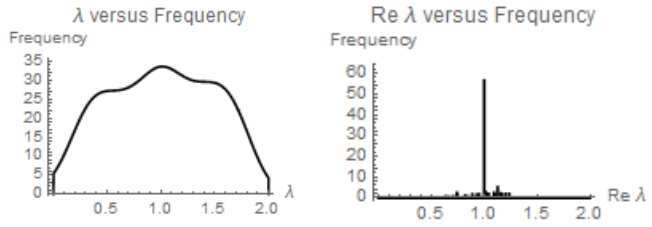

(c) 100 nodes BA

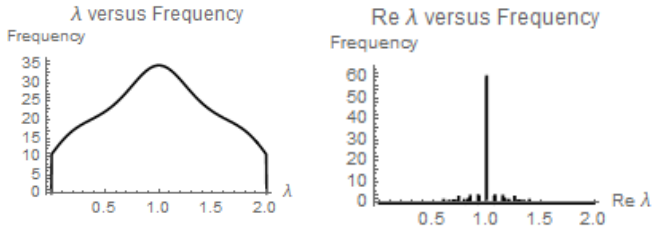

(d) 100 nodes S_{grid}

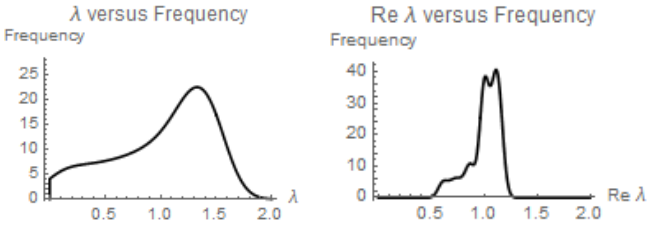

(e) 105 nodes T_{grid}

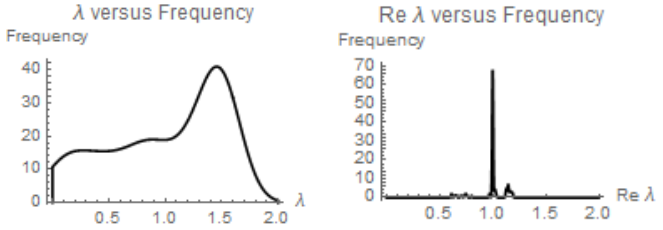

(f) 116 nodes GGN

Figure 10. Spectral Plots for Undirected (left) and Directed (right) Network Models

From the spectral plots, we found that the peaks are at around eigenvalue 1 to 1.5 for the undirected and 1 for the directed connection. Spectral plots for the directed network models do not show much variety as compared to the undirected one when the number of nodes increases. The main reasons for having all these features can be uncovered using network motifs. Motifs are considered simple building blocks of complex networks (Wong, 2011) or patterns that recurred in many parts of the network (Abedijaberi, 2018). In this work, small graphs were created in motif form as shown in Figures 9 to investigate these eigenvalues. These kinds of motif were found to have a high repetition rate in the network models.

From Figure 9(a), (f), (g) and (h), we can see that whenever there is an addition or duplication of nodes, eigenvalue 1 increases. Since ER network model has a high eigenvalue around 1 in the spectrum, this indicates that ER network has a very high tendency to be formed from the combination of tree motif and bipartite motif.

For WS network model, since each node connects to two of its nearest neighbour, most of the nodes do not have a high degree but instead have many cliques that produce fewer

eigenvalue 1. NLSPD of WS network models from Figure 10(b) showed a lower hump at 0.3 and upper hump at 1.4. The possible explanation of this was due to the occurrence of clique-type motifs as shown in Figure 9 where their eigenvalues do not focused at eigenvalue 1.

For BA spectral plot (Figure 10(c)), it shows a sharp peak at eigenvalue 1 and two smaller humps at eigenvalue 0.5 and 1.5. The Bow-tie motif in Figure 9 produced eigenvalues 0.5 and 1.5 hence there is high possibility BA networks have a lot of bow-tie motifs. Since BA model satisfied the scale-free characteristics where there emerge nodes with high degrees, tree and bipartite motifs are also part of its building blocks.

The S_{grid} network model has shown a smooth NLSPD for n= 100, but when the nodes increase, hump were seen at the slopes around eigenvalue 0.5 and 1.5. These humps are formed if the horizontal expansion is more than the vertical one. The square motif appear is clear as it produces eigenvalues around 0 2, 1.6, 1.6, 1, 1, 0.4, 0.4 and 0 as clearly shown in Figure 9(i).

For T_{grid} network model, the peak of the eigenvalue shifted toward eigenvalue 1.4. This peak is formed mainly due to the abundance of clique-type motifs (triangle motifs) in the network. As can be seen in Figure 9, the triangle motif produces a lot of eigenvalue around 1.5. As for GGN, the high peak around eigenvalue 1.5 means that GGN consist of a lot of triangle motif. Besides only triangle motifs, GGN network models also consist of motifs (c), (d) and (e) as shown in Figure 9. As a result, the spectral plot is not exactly like the T_{grid} but with some smaller peaks between 0.2 to 1.5.

As for the directed network, the computed eigenvalues are in complex numbers where only the real part are used for the plots. When directions are added to some of the undirected network motifs as can be seen in Figure 11, the eigenvalues changed because of the direction flow. As can see from Figure 11(a) to (d), open loop and closed loop non-cyclic motifs can produce many eigenvalues 1 while the cyclic motif Figure 11(e) to (i) usually will produce a mixture of eigenvalues.

From the spectral plots, as shown in Figure 10, all the networks have smaller distribution widths and sharp peaks at eigenvalues 1 except T_{grid} where the sharp peak is at eigenvalues 1 and 1.2. Having a sharp peak at eigenvalue 1 implies that most of the connection is acyclic and depends on motif addition and duplication Figure 11(a) to (d). Since the building block of T_{grid} is a triangle, it has a greater chance to form motifs as in Figure 11(c) to g) hence giving rise to peak at eigenvalue 1.2.

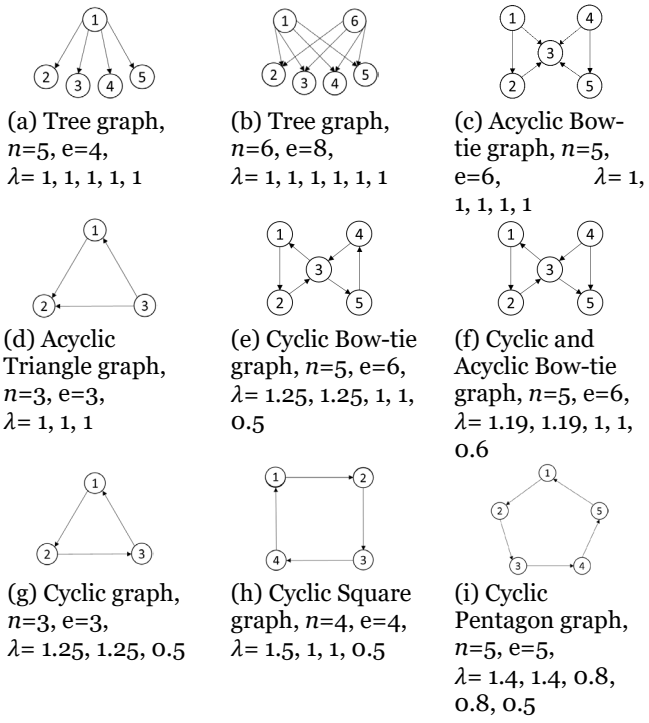

(a) Tree graph, n=5, e=4, λ= 1, 1, 1, 1, 1

(b) Tree graph, n=6, e=8, λ= 1, 1, 1, 1, 1, 1

(c) Acyclic Bow-tie graph, n=5, e=6, λ= 1, 1, 1, 1, 1

(d) Acyclic Triangle graph, n=3, e=3, λ= 1, 1, 1

(e) Cyclic Bow-tie graph, n=5, e=6, λ= 1.25, 1.25, 1, 1, 0.5

(f) Cyclic and Acyclic Bow-tie graph, n=5, e=6, λ= 1.19, 1.19, 1, 1, 0.6

(g) Cyclic graph, n=3, e=3, λ= 1.25, 1.25, 0.5

(h) Cyclic Square graph, n=4, e=4, λ= 1.5, 1, 1, 0.5

(i) Cyclic Pentagon graph, n=5, e=5, λ= 1.4, 1.4, 0.8, 0.8, 0.5

Figure 11. Various Motifs with cyclic or acyclic flow (n=number of nodes, e=number of edges and λ={eigenvalues})

Table 2. Basic measures for undirected network models

Network Models	Number of Vertex	Number of Edges	Density	Total number of Degree	Mean Degree	Mean Deviation	Average Path Length	Average Clustering Coefficient
ER	100	990	0.20	1980.00	19.80	2.91	1.81	0.20
	300	8970	0.20	17940.00	59.80	5.49	1.80	0.20
	500	24950	0.20	49900.00	49.90	7.03	1.80	0.20
	1000	99900	0.20	199800.00	199.80	9.80	1.80	0.20
WS	100	200	0.04	400.00	4.00	0.66	4.16	0.24
	300	600	0.01	1200.00	4.00	0.61	5.36	0.24
	500	1000	0.01	2000.00	4.00	0.58	5.99	0.26
	1000	2000	0.002	4000.00	4.00	0.49	7.05	0.28

BA	100	197	0.04	394.00	3.94	2.18	3.02	0.20
	300	597	0.01	1194.00	3.98	2.37	3.77	0.05
	500	997	0.01	1994.00	3.99	2.40	3.72	0.05
	1000	1997	0.00399	3994.00	3.99	2.33	4.10	0.02
S_{grid}	100	180	0.02	360.00	3.60	0.51	6.67	0.00
	300	560	0.01	1120.00	3.73	0.40	13.33	0.00
	500	940	0.00376	1880.00	3.76	0.37	20.00	0.00
	1000	1890	0.00189	3780.00	3.78	0.35	36.67	0.00
T_{grid}	105	273	0.05	546.00	5.20	1.06	3.00	0.45
	210	570	0.03	1140.00	5.43	0.83	3.38	0.43
	528	1488	0.01	2976.00	5.64	0.60	3.91	0.42
	1035	2970	0.00278	5940.00	5.74	0.46	4.30	0.41
GGN	116	228	0.03	456.00	3.93	1.50	3.52	0.64
	373	762	0.01	1524.00	4.09	1.61	4.24	0.64
	545	1116	0.01	2232.00	4.10	1.63	4.50	0.64
	1150	2376	0.00179	4752.00	4.13	1.66	4.97	0.63

For GGN models, we can see a left shift for the peak eigenvalue in the directed network shown in Figure 10 as compared to the undirected one. The main reason for this shifting towards eigenvalue 1 is the high number of acyclic motif, as this motif is much easier to form than the cyclic one.

D. Cheeger Constant

Cheeger constant (h_G) is a numerical measure used to check whether a graph has a bottleneck, i.e. a point where the system is limited by connection (Butler, 2016). h_G is related to the spectral gap, namely the second smallest eigenvalues from the spectrum where it is bounded by the Cheeger Inequalities. Cheeger Inequalities is used to calculate the lower and upper boundaries for the eigenvalues of the networks.

The h_G is affected by two crucial factors, namely edges that are needed to be removed and the ratio of the volume of subsets. The value of h_G becomes larger when more edges are removed. This actually implied that the network is more difficult to be separated. If ratio vol S : vol $\bar{S}$ is 1, this means that the division of the subset is balanced; subset S is equal to the subset $\bar{S}$. If it is minimal then, it is a highly unbalanced where subset S is very small and subset $\bar{S}$ is very big. From our calculation, h_G for undirected and directed networks are the same.

The ER network model produces high second eigenvalues (Figure 12) as compared to other networks, this means that it is difficult to be separated into two subgroups. The results displayed in Figure 12 are results that have been filtered where subgroups with only one node are ignored, and the smallest h_G is chosen.

From Figure 12, we found that the spectral gap for all network models decreased when the number of nodes increased except for ER network model. This happened because ER network model is a random network with low clustering among the nodes. It is more difficult to separate this network into subgroups and the increase in the spectral gap is consistent with the h_G values as it increases from 0.37 to 0.47 for 100 to 500 nodes respectively.

This is not the case for other network models as h_G changes less than 0.09 as the number of nodes increases. This implied that these network models are well clustered and can have many subgroups which might affect the h_G calculation. An increase in the number of nodes does not affect much on separating the network into two subgroups because there is an infinite number of ways to separate the graph into two.

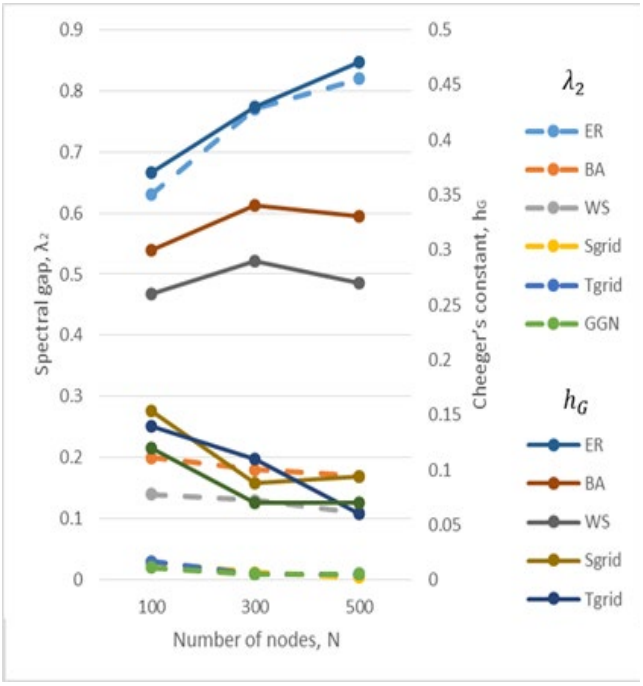

Figure 12. Cheeger constant (h_G) and spectral gap (λ_2) against the number of nodes (n)

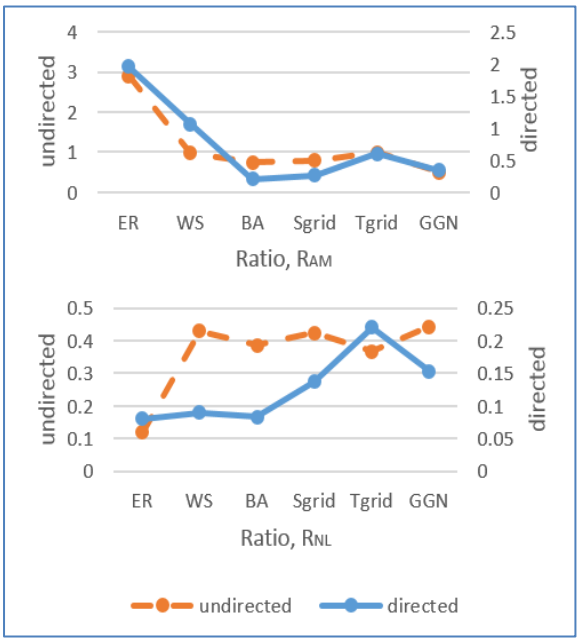

Figure 13. Ratio, R_{AM} and R_{NL} of undirected and directed network models

F. Energy Measurement

The topology structure of an undirected and directed network can be determined by looking at the energy ratio, R_{AM} and R_{NL} computed based on the energy of *A(G)* and *NL(G)* respectively.

From the Table 3 and 4, we found that the undirected T_{grid} network with 528 nodes and all undirected and directed ER network models have R_{AM} higher than 1. According to Koolen *et al.* (2000), if adjacency matrix energy is greater than 2*n*-2, they are called a hyper-energetic network i.e. strongly regular graphs (Jahanbakht, 2010) or highly random strongly regular graphs (Cameron, 2003) with the number of edges several multiple higher than its number of nodes. Since the edges generated in ER network are based on probability ($p = 0.2$, in our generation), we can say it is a highly random network.

For WS, BA, S_{grid}, T_{grid} and GGN, the average R_{AM} for both undirected and directed networks are computed as (0.980, 1.060), (0.742, 0.204), (0.785, 0.264), (0.984,0.597) and (0.502, 0.338) respectively as shown in Figure 13. These values do not change much as the network size increases. This might be due to the number of edges increase linearly with the increases of nodes except for ER which increases exponentially.

$R_{AM}(G)$ for WS and T_{grid} are higher than BA and S_{grid} mainly because they tend to form cliques and nodes do not have a very high degree. In contrast to BA, some of the nodes might have a very high degree but since edges are limited, some of the nodes have a low degree implying that it is more spread out. As for S_{grid}, since the number of degrees of each node represents how they are clustered, S_{grid} has fewer degrees than T_{grid}, hence having lower $R_{AM}(G)$. As for GGN, it shows that it has balanced clustered nodes as well as nodes with low degrees.

As for *NL(G)*, it is found that energy for a complete network $E_{NL}(G)$ and $E_{NL}(\bar{G})$ tends to converge to 2 and 1 respectively. Almost all the R_{NL} remain constant because the energy is linearly correlated with the network size except for ER model which has a noticeable decrease. The reason for the decrease is due to the exponential increase in edges which causes the network to have a high clustering amongst the nodes.

As for the directed part, the $E_A(\bar{G})$ and $E_{NL}(\bar{G})$ both have an opposite trend. When R_{AM} goes up, R_{NL} will go down and is consistent with the increased network size for both connectivity matrices. $R_{AM}(\bar{G})$ depend highly on cycles on the digraph. If the digraph has no cycle (acrylic graph) $E_A(\bar{G}) = 0$ (Pena & Rada, 2008). Figure 14 shows some energy of the motif that has been used here.

(a)

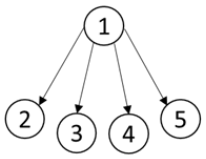

$E_A(\bar{G}) = 0.00$

$E_{NL}(\bar{G}) = 0.00$

(b)

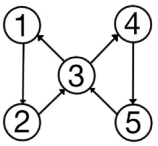

$E_A(\bar{G}) = 2.52$

$E_{NL}(\bar{G}) = 1.00$

(c)

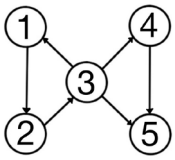

$E_A(\bar{G}) = 2.00$

$E_{NL}(\bar{G}) = 0.79$

(d)

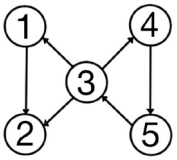

$E_A(\bar{G}) = 0.00$

$E_{NL}(\bar{G}) = 0.00$

Figure 14: Energy of motif with directed links

We can see that 13(a) and 13(d) are acyclic hence the $E_A(\bar{G})$ and $E_{NL}(\bar{G})$ are zero whereas for Figure 14(b) where the motif has 2 cycles, the energy is 2.52 and 1.00. For Figure 14(c), there is only one cycle, hence the energy is reduced to 2.00 and 0.79. For $E_{NL}(\bar{G})$, it can have a value of less than 1 if the network is not perfectly cyclic.

With this in mind, when we compare the energy between directed and undirected, the values are greatly reduced because open-loop motifs that appear in the directed networks contribute no energy to the system while only those with cyclic close-loop counts. It is understood that those with closed-loop means that they are networks that are highly clustered together such as WS, ER and T_{grid}. ER has the highest energy mainly because it has many edges for connection and as such produces more cycles than others while T_{grid}, has the most basic triangle motif in its structure to form a cycle. For BA and S_{grid}, the energy tends to be lower than the others mainly because BA has hubs and many nodes have lower degrees while S_{grid}'s square motif has a lower probability to form a cycle.

Table 3. Energy and ratio R_{AM} of undirected and directed network model using $A(G)$

Network Model	**Energy for undirected network, $E_{NL}(G)$**			**Energy for directed network, $E_A(\bar{G})$**		
	100	**300**	**500**	**100**	**300**	**500**
Complete Network	198	598	998	98.08	298.04	498.10
ER	353.13	1814.86	3879.24	119.03	610.16	1311.00
Ratio, R_{AM}	1.78	3.03	3.89	1.21	2.04	2.63
WS	196.78	582.55	973.09	105.93	316.95	525.44
Ratio, R_{AM}	0.99	0.97	0.98	1.08	1.06	1.05
BA	149.73	451.09	713.33	21.18	46.11	120.82
Ratio, R_{AM}	0.76	0.75	0.72	0.22	0.16	0.24
S_{grid}	153.50	472.72	787.47	27.31	75.93	128.58
Ratio, R_{AM}	0.78	0.79	0.79	0.28	0.26	0.26
	105	**210**	**528**	**105**	**210**	**528**
Complete Network	208	418	1054	102.808	207.818	526.001
T_{grid}	201.14	411.28	1054.73	62.58	117.00	325.81
Ratio, R_{AM}	0.97	0.98	1.00	0.61	0.56	0.62
	116	**373**	**545**	**116**	**373**	**545**
Complete Network	230	744	1088	114.08	371.05	543.04
GGN	116	373	545	35.24	126.56	197.04
Ratio, R_{AM}	0.50	0.50	0.50	0.31	0.34	0.36

IV. CONCLUSION

In this work, we have managed to construct six network models namely ER, WS, BA, S_{grid}, T_{grid} and GGN with undirected and directed connections using Mathematica with a varied number of nodes. The spectrum of *NL(G)* has been computed for each network model and was analysed using spectral plots, Cheeger constant and energy measurement.

From NLSDP, it has revealed that the different undirected network models, showed very different patterns which can be easily recognised. Since complexity increases when the network grows bigger, network such as ER, WS and BA become very difficult to be recognised and classified. However, from the spectral plots, the pattern remains consistent when the number of nodes increased from 100 to 500. For directed network models, most of the models showed a very sharp peak at eigenvalue 1 except for T_{grid} and GGN, which have a small and a sharp peaks feature. The unique plot pattern in the network models can be explained and analysed using network motifs. Since different graph motifs produced distinct eigenvalues, the addition or multiplication of them affects the patterns of spectral density plots. Models that have a sharp peak at eigenvalue 1 are expected to have tree type and bipartite motifs as the main building block, while those having other peaks beside 1 have a combination of clique-type motifs. In the directed plots, eigenvalues are mainly affected by whether the motif is cyclic or noncyclic and whether they are open or closed loops. Motifs with open loop and noncyclic closed loop produced a high number of eigenvalue 1, while those with closed loop and cyclic can produced a different range of eigenvalues.

Cheeger constant (h_G) measurement does not consider direction hence undirected and directed connections produce a similar result. From the measurement, ER models have the highest h_G followed by BA and WS. Having high h_G imply that it is much harder to be separated due to the high volume of edges and random distribution of its edges. As the number of nodes increases, h_G increased for ER model.

In the energy measurement, $A(G)$ and $NL(G)$ are used in both undirected and directed network models. A comparison between energy measurement using $A(G)$ and $NL(G)$ have shown that both ratios for WS, BA, S_{grid}, T_{grid} and GGN do not change much as the network size increase mainly because the edges increase linearly with the numbers of nodes. Energy measurement for the directed networks shows that the energy

Table 4. Energy of undirected and directed network model using normalised Laplacian $NL(G)$

Network Model	**Energy for undirected, $E_{NL}(G)$**			**Energy for directed network, $E_{NL}(\overline{G})$**		
	100	**300**	**500**	**100**	**300**	**500**
Complete Network	2	2	2	0.99	1.00	1.00
ER	18.03	30.48	38.97	6.12	10.26	13.21
Ratio, R_{NL}	0.18	0.10	0.08	0.12	0.07	0.05
WS	42.61	128.03	213.8	9.14	27.19	43.15
Ratio, R_{NL}	0.43	0.43	0.43	0.09	0.09	0.09
BA	40.17	118.43	186.44	3.97	8.63	27.02
Ratio, R_{NL}	0.40	0.39	0.37	0.08	0.06	0.11
S_{grid}	43.26	126.65	211.27	7.18	19.81	33.84
Ratio, R_{NL}	0.43	0.42	0.42	0.14	0.13	0.14
	105	**210**	**528**	**105**	**210**	**528**
Complete Network	2	2	2	1.0	1.0	0.98
T_{grid}	39.46	76.91	189.00	12.04	21.71	58.19
Ratio, R_{NL}	0.38	0.36	0.36	0.23	0.21	0.22
	116	**373**	**545**	**116**	**373**	**545**
Complete Network	2	2	2	1.0	1.0	1.0
GGN	52.23	164.81	240.30	8.12	28.16	47.15
Ratio, R_{NL}	0.45	0.44	0.44	0.14	0.15	0.17

is much smaller than the undirected part because it depends on closed-loop network. Open-loop and acyclic networks give zero energy value to the system.

For future research, the spectral analysis can be performed on real-world networks because the spectral analysis in this work is limited to network models.

V. ACKNOWLEDGEMENT

The authors wish to acknowledge the financial support provided through the Fundamental Research Grant Scheme (FRGS), Project No. FRGS/1/2020/STG07/UPM/02/2 by Ministry of Higher Education Malaysia.

VI. REFERENCES

Abedijaberi, A 2018, 'Motif-level Robustness Analysis of Power Grids', IEEE International Conference on Data Mining Workshops (ICDMW).

Andreopoulos, W & Labudde, D 2003, 'Protein-protein interaction networks', Science, vol. 302, pp. 353-353.

Balakrishnan, R 2004, 'The energy of a graph', Linear Algebra and its Applications, vol. 387, pp. 287–295.

Banerjee, A 2008, 'The Spectrum of the Graph Laplacian as a Tool for Analyzing Structure and Evolution of Networks', Ph.D. dissertation, Faculty of Mathematics and Computer Science, University of Leipzig.

Barabasi, AL & Albert, R 1999, 'Emergence of scaling in random networks', Science, vol. 286, pp. 509—512.

Butler, S 2016, 'Algebraic aspects of the normalized Laplacian', The IMA Volumes in Mathematics and its Applications, vol. 159, Springer, Cham.

Cameron, PJ 2003, 'Strongly regular graphs', Discrete Mathematics, vol. 273, no. 1, pp. 103–114.

Castro, R & Grossman, J 1999, 'Famous trails to Paul Erdos. With a sidebar by Paul M. B. Vitanyi', The Mathematical Intelligencer, vol. 21.

Cavers, M, Fallat, S & Kirkland, S 2010, 'On the normalized Laplacian energy and general Randic index R_{-1} of graphs', Linear Algebra and its Applications, vol. 433, no. 1, pp. 172-190. ISSN 0024-3795.

Chung, FR 1997, 'Spectral Graph Theory', Conference Board of the Mathematical Sciences.

Erdos, P & Renyi, A 1959, 'On random graphs', Publicationes Mathematicae 6, pp. 290-297.

Ernesto, E, Matthias, D & Frank, E-S (eds) 2009, 'Spectral Theory of Networks: From Biomolecular to Ecological Systems', in Analysis of Complex Networks, pp. 55-83.

Koolen, JH, Moulton, V & Gutman, I 2000, 'Improving the McClelland Inequality for Total π-Electron Energy', Chemical Physics Letters, vol. 320, pp. 213-216.

Jahanbakht, N 2010, 'Energy of graphs and digraphs', University of Lethbridge, Faculty of Arts and Science.

Li, Y & Zhang, Z-L 2015, 'Understanding Complex Networks Using Graph Spectrum', Florence, Italy. ACM 978-1-4503-3473-0/15/05.

Li, Y, Shang, Y & Yang, Y, 2017, 'Clustering coefficients of large networks', Information Sciences, vol. 382, pp. 350-358. ISSN 0020-0255.

Liang, YSJ, Chan, KT, Zainuddin, H & Shah, NM 2019, 'Extracting Network Structure for International and Malaysia Website via Random Walk', ASM Science Journal. vol. 12, pp. 1-10. doi: 10.32802/asmscj.2019.400.

Mislove, AE 2009, 'Online Social Networks: Measurement, Analysis, and Applications to Distributed Information Systems', Rice University.

Newman, ME 2004, 'Detecting community structure in networks', Eur. Phys. J. B, vol. 38, pp. 321-330.

Newman, ME 2010, 'Networks: an introduction', Oxford; New York: Oxford University Press.

Pantazopoulos, P 2015, 'Internet Content Management using Complex Network Analysis techniques', PhD thesis, National and Kapodistrian University of Athens.

Pattanayak, HS, Verma, HK, & Sangal, AL 2020, 'Lengthening of average path length in social networks due to the effect of community structure', Journal of King Saud University - Computer and Information Sciences.

Polya, G & Szego, S 1951, 'Isoperimetric Inequalities in Mathematical Physics', Annals of Math. Studies, no. 27, Princeton University Press.

Rada, J 2009, 'The McClelland inequality for the energy of digraphs', Linear Algebra and its Applications, vol. 430, no. 2, pp. 800–804.

Sarkar, C & Jalan, S 2018, 'Spectral properties of complex networks', Chaos: An Interdisciplinary Journal of Nonlinear Science, vol. 28, no. 10, p. 102101.

Taha, MH, Tim, CK & Zainuddin, H 2016, 'Construction of Network Based on Modular group', The Malaysian Solid State Science and Technology Society.

Watts, D & Strogatz, S 1998, 'Collective dynamics of 'small-world' networks', Nature, vol. 393, pp. 440–442.

Weisstein, EW 2001, 'Grid Graph', MathWorld- A Wolfram Web Resource, <https://mathworld.wolfram.com/GridGraph.html>.

Wong, E 2011, 'Biological network motif detection: principles and practice', Briefings in Bioinformatics, vol. 13, no 2, pp. 202-215.

Wu, Z, Menichetti, G, Rahmede, C & Biaconi, G 2014, 'Emergent Complex Network Geometry', Scientific Reports.